

Supplementary Materials

**Reexamination of the structure of nanomineral opal-CT using
synchrotron X-ray diffraction, transmission electron microscopy, X-
ray scattering structure factor and pair distribution function
analyses**

Seungyeol Lee^{1,2}, Huifang Xu^{1,*}, Hongwu Xu³, and Wenqian Xu⁴

¹Department of Geoscience, University of Wisconsin–Madison, Madison, WI 53706, USA

²Department of Earth and Environmental Sciences, Chungbuk National University, Cheongju
28644, Republic of Korea

³School of Molecular Sciences and Center for Materials of the Universe, Arizona State
University, Tempe, AZ 85287, USA

⁴X-ray Science Division, Advanced Photon Source, Argonne National Laboratory, Argonne, IL
60439

* Corresponding author: hfxu@geology.wisc.edu

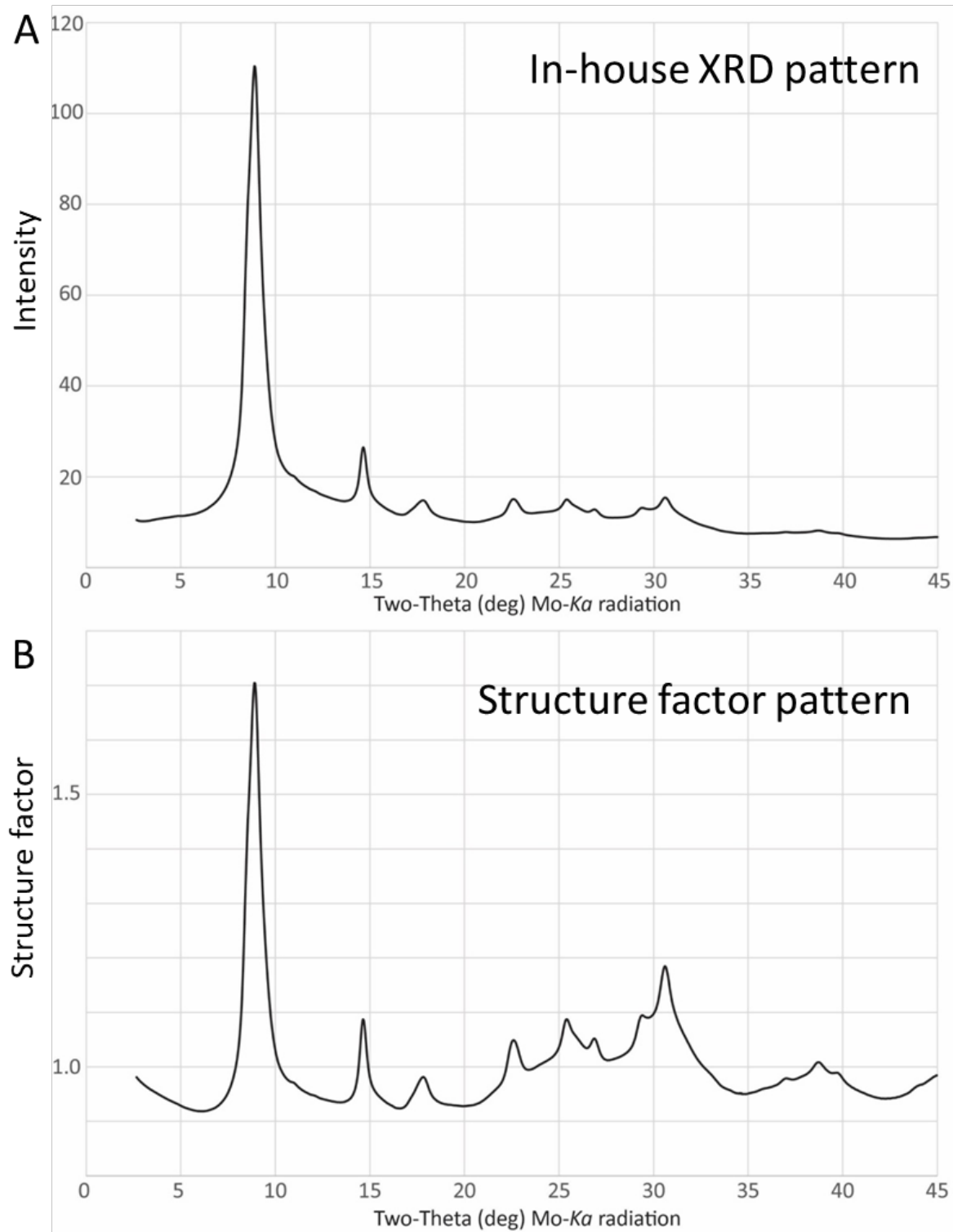


Figure S1. (A) Laboratory XRD pattern of opal-CT(1) and (B) its X-ray scattering structure factor $S(Q)$ pattern.

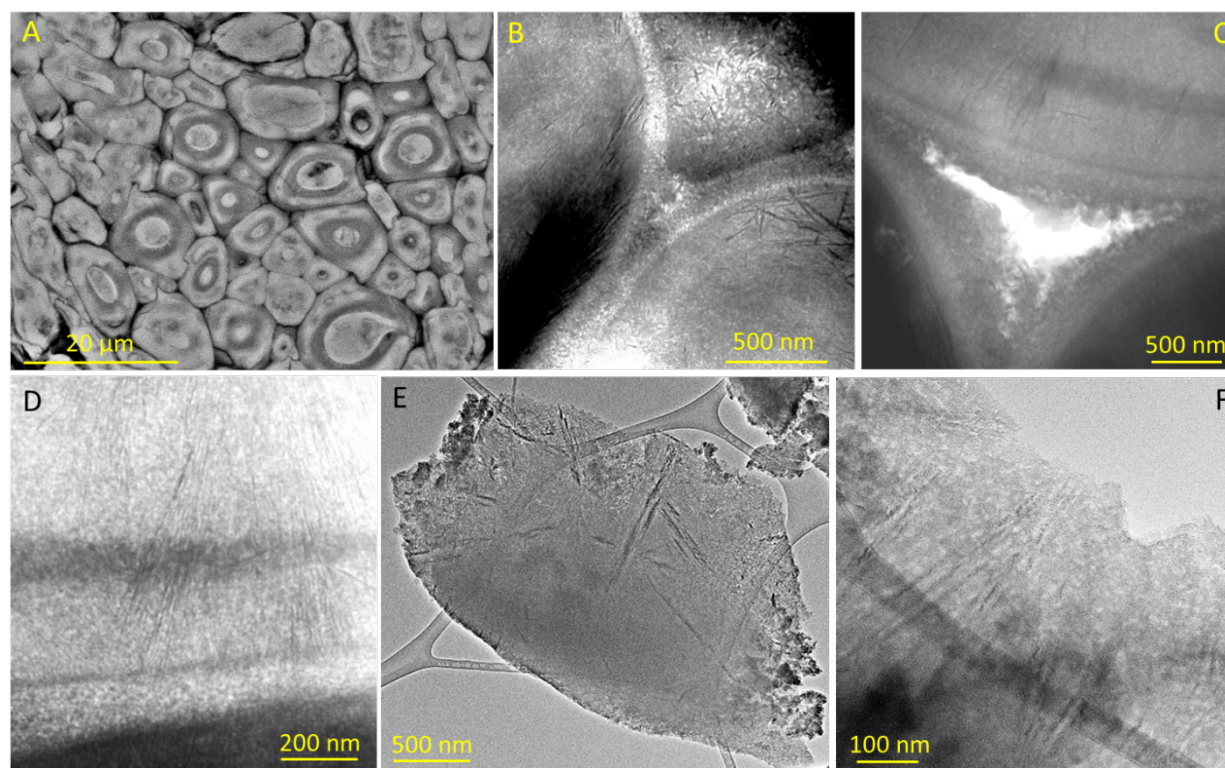


Figure S2. (A) SEM-BSE image and (B-F) bright-field TEM images of opal-CT (2) collected from a petrified wood slab in Arizona, USA. The intensity difference in the SEM image is due to porosity or density variations in different areas.

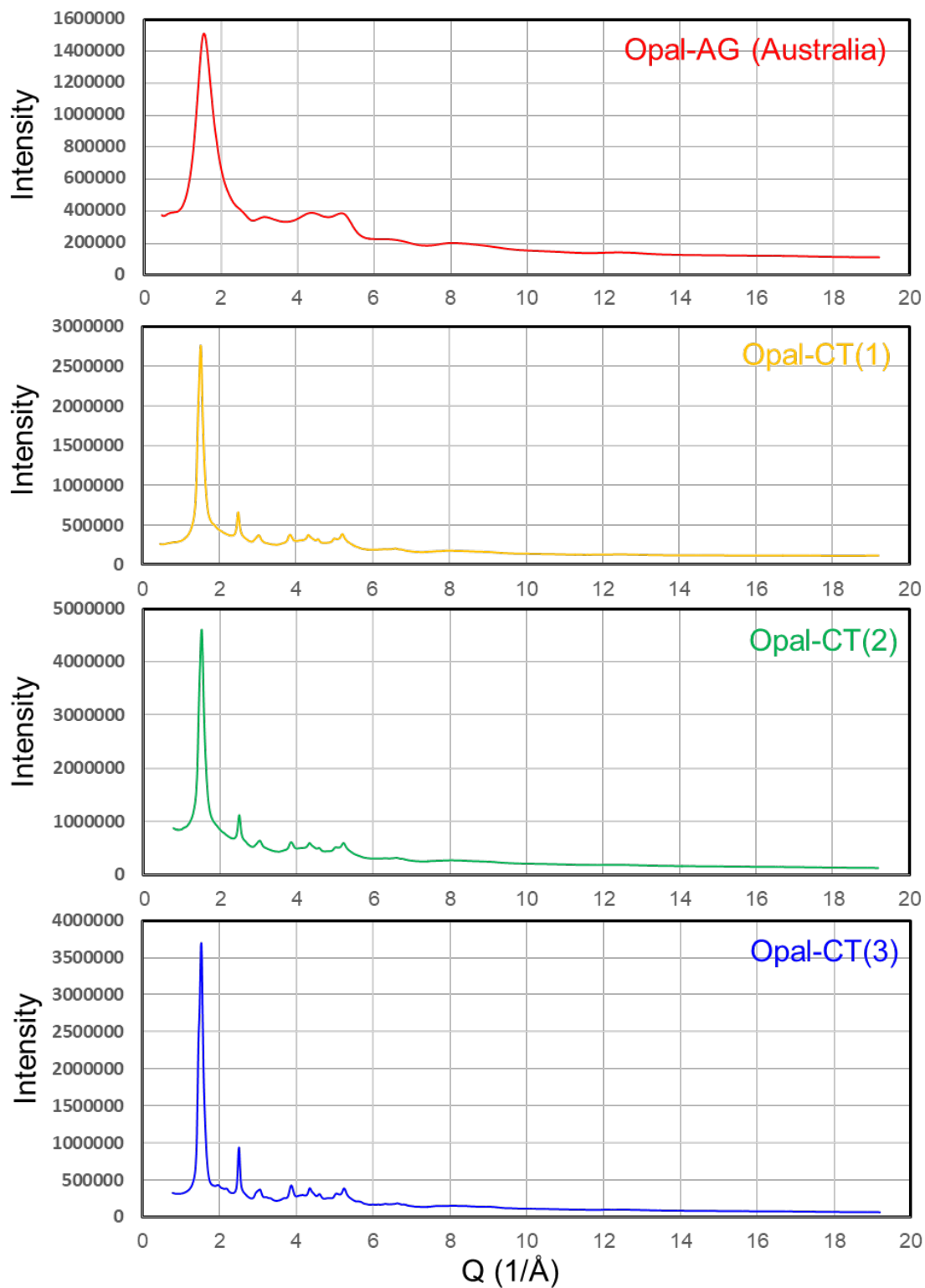


Figure S3. $I(Q)$ patterns of the three opal-CT and an opal-AG samples up to Q_{max} of 19.1 \AA^{-1} .

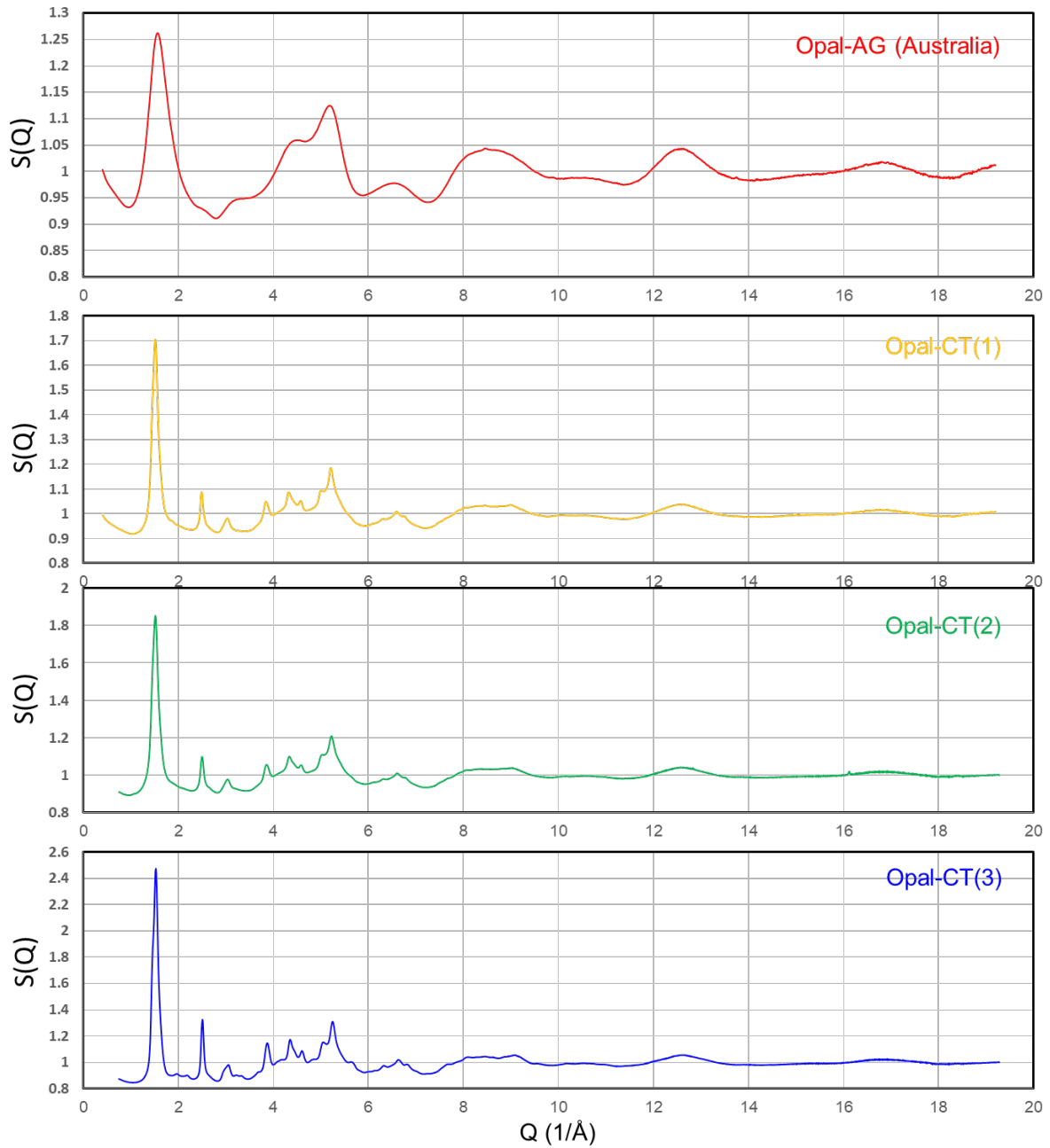


Figure S4. X-ray scattering structure factor $S(Q)$ patterns of the three opal-CT and an opal-AG samples up to Q_{max} of 19.1 \AA^{-1} .

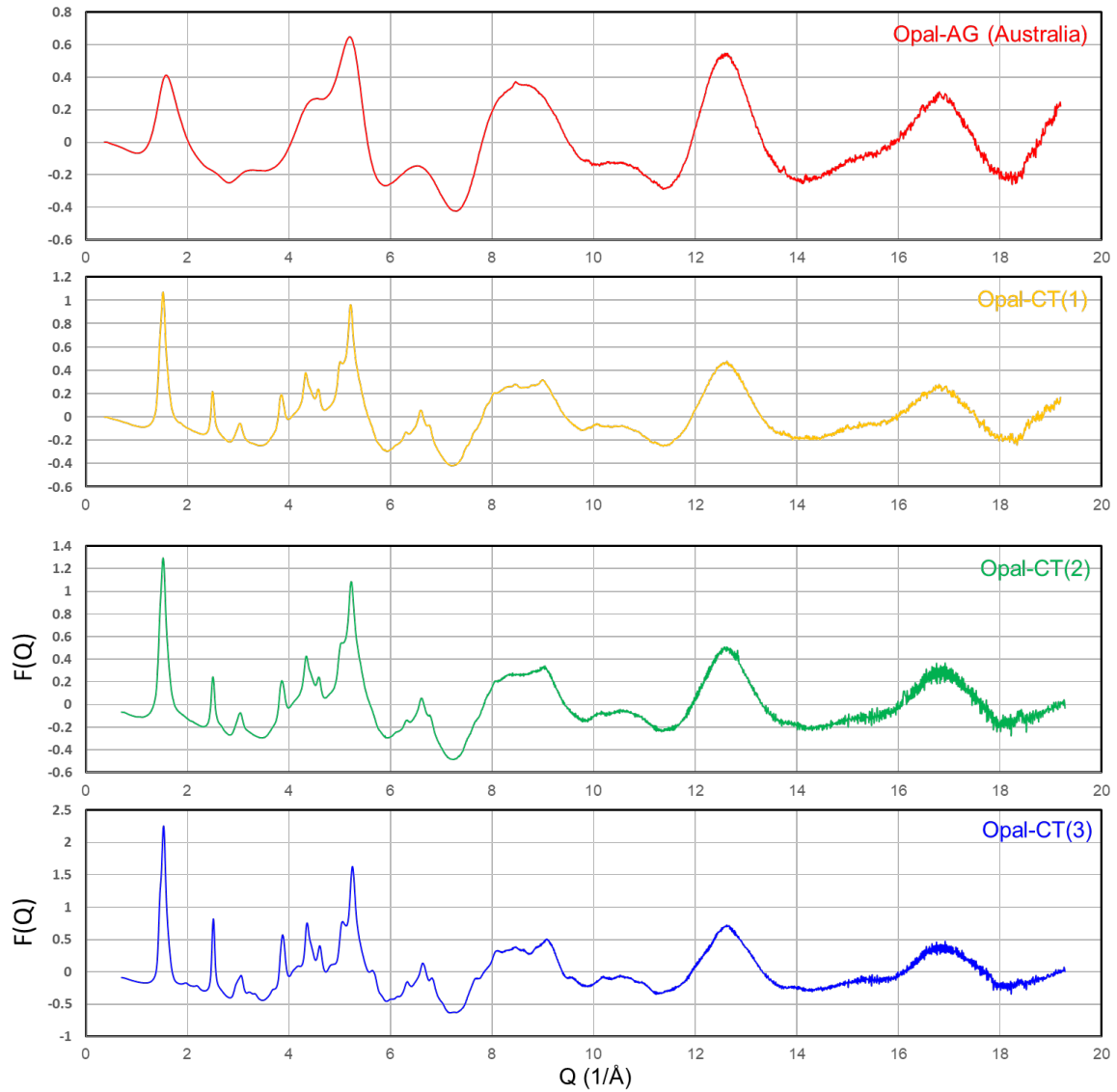


Figure S5. $F(Q)$ patterns of the three opal-CT and an opal-AG samples up to Q_{max} of 19.1 \AA^{-1} .

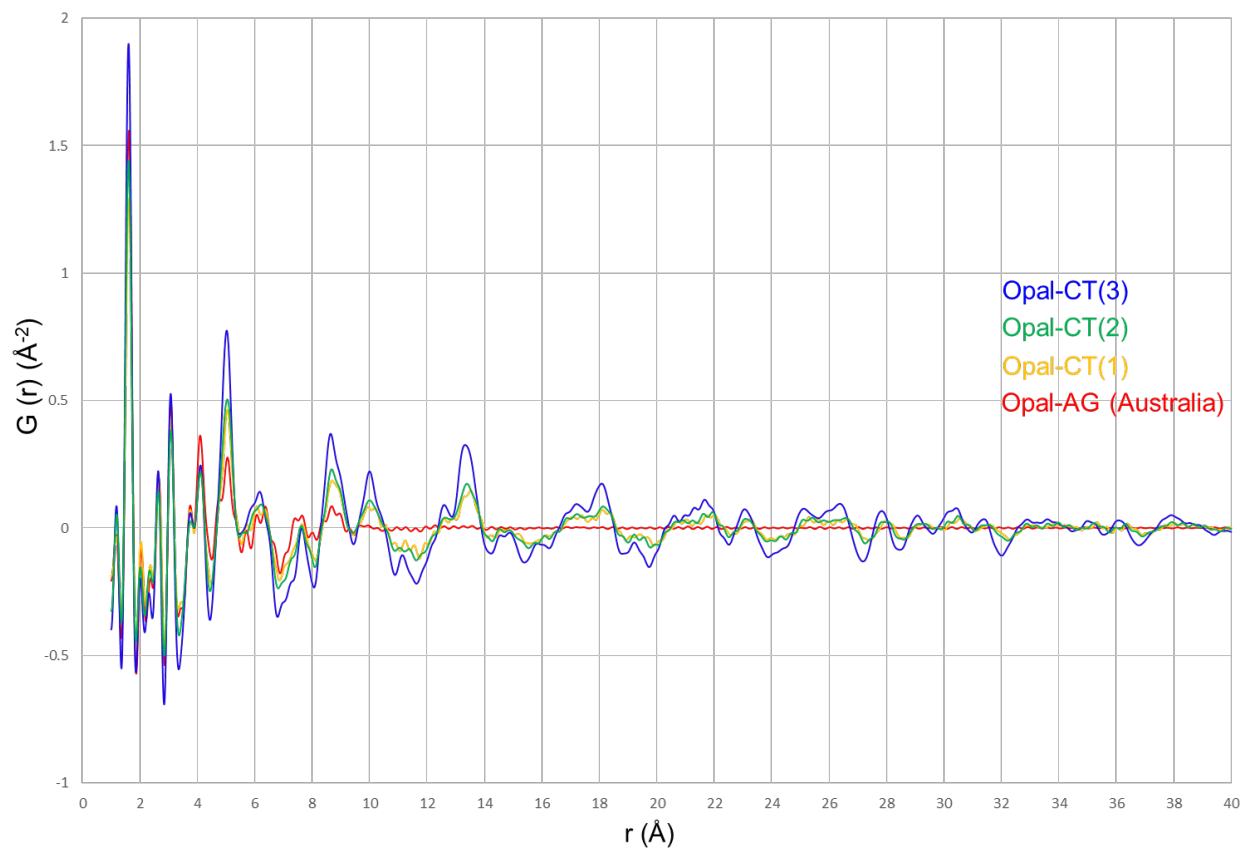


Figure S6. PDF pattern, $G(r)$, of the three opal-CT and an opal-AG samples from 1 to 40 \AA .

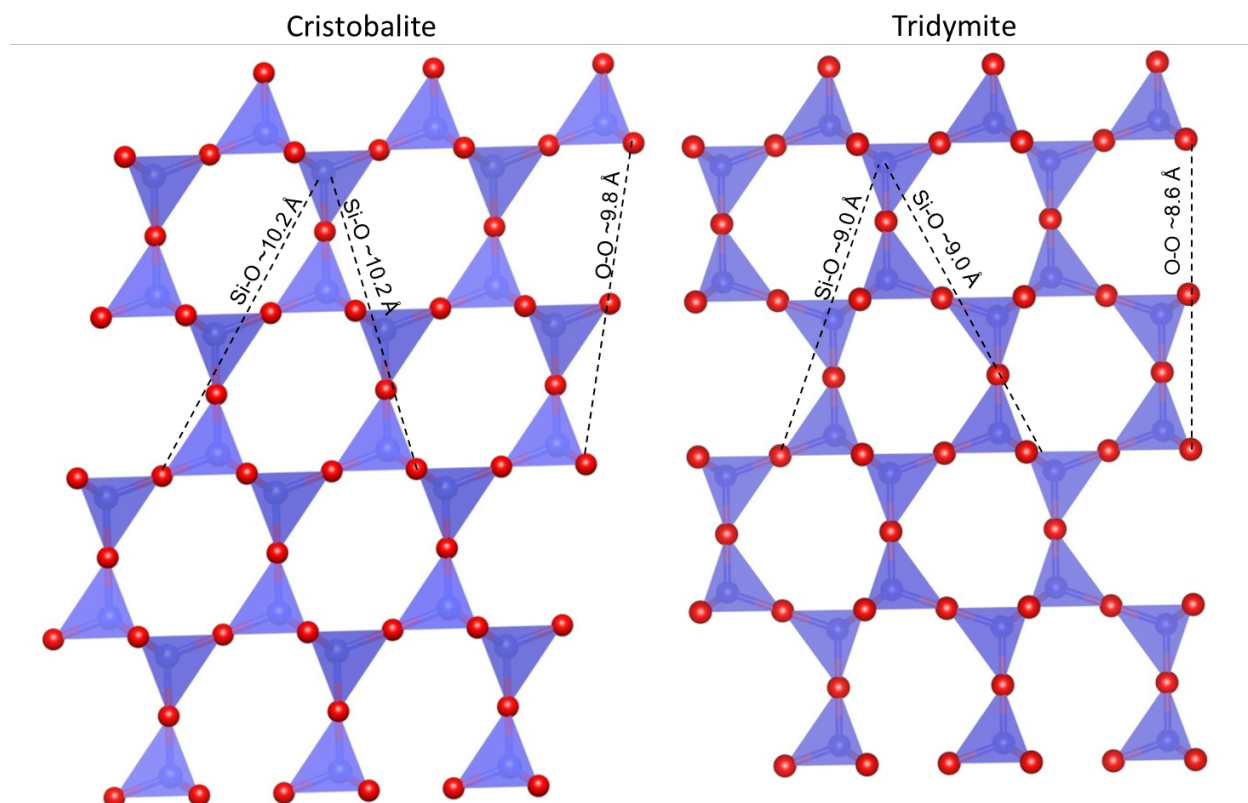


Figure S7. A schematic representation of stacking fault models producing the distinct cristobalite peak at 10.0–10.2 Å, where the tridymite structure contributes minimally.

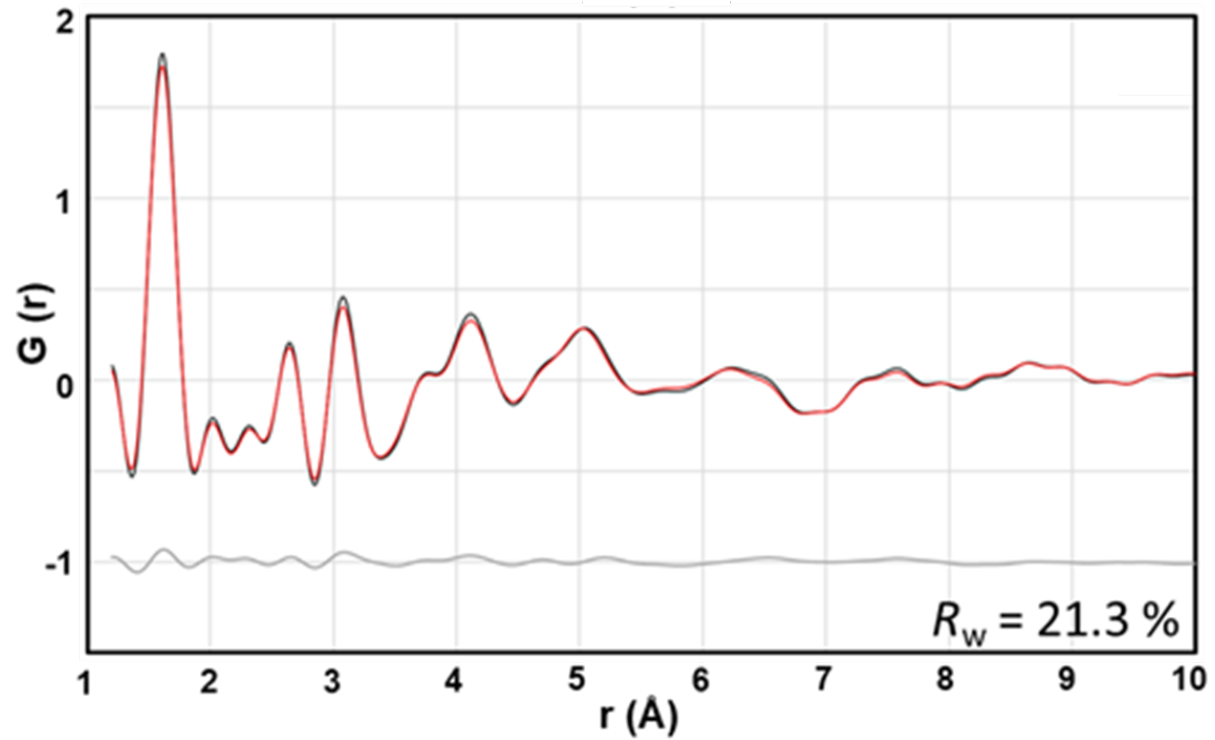


Figure S8. PDF refinement of opal-A using models of cristobalite and tridymite (Lee and Xu 2019), interstratified phase, and twin boundary model.

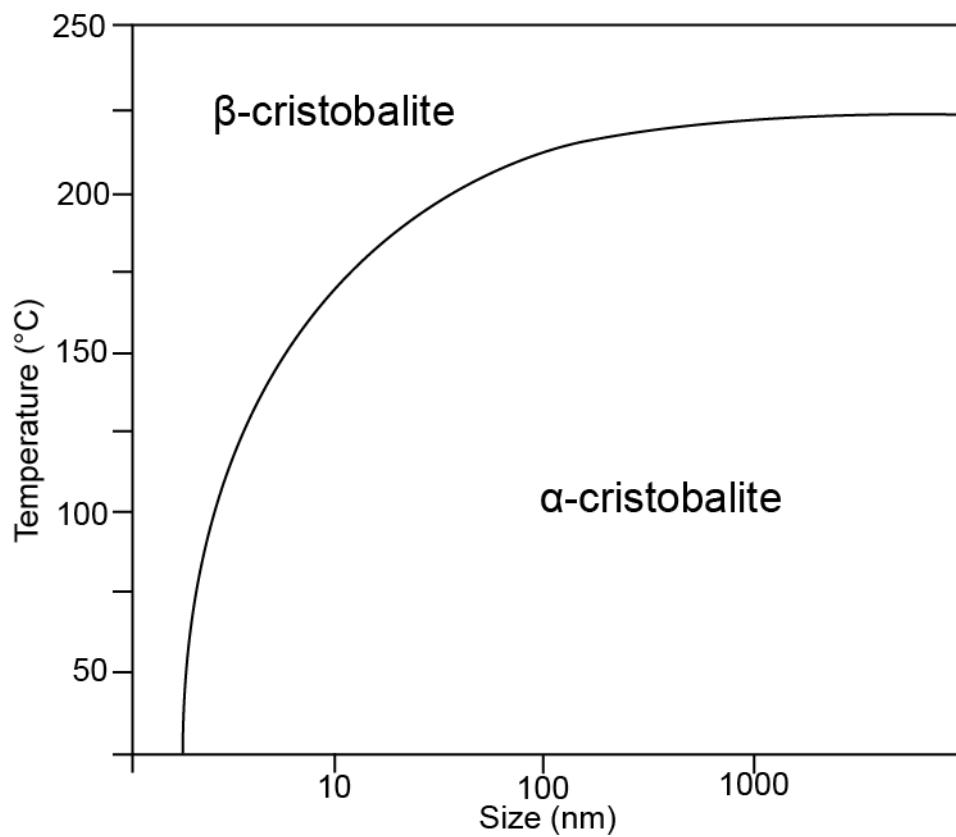


Figure S9. A schematic diagram of the size-dependant α - β phase transition in cristobalite designed from Hatch and Ghose (1991) and Hill et al. (2019).

References

- Hatch, D. M., & Ghose, S. (1991). The α - β phase transition in cristobalite, SiO₂: Symmetry analysis, domain structure, and the dynamical nature of the β -phase. *Physics and Chemistry of Minerals*, 17(6), 554-562.
- Hill, T. R., Konishi, H., Hobbs, F., Lee, S., & Xu, H. (2019). Precipitates of α -cristobalite and silicate glass in UHP clinopyroxene from a Bohemian Massif eclogite. *American Mineralogist*, 104(10), 1402-1415.
- Lee, S., and Xu, H. (2019) Using powder XRD and pair distribution function to determine anisotropic atomic displacement parameters of orthorhombic tridymite and tetragonal cristobalite. *Acta Crystallographica Section B: Structural Science, Crystal Engineering and Materials*, 75, 160–167.